

Antioxidant Additives Produced from Argan Shell Lignin Depolymerization

Zainab Afailal, Noemí Gil-Lalaguna, María Teresa Torrijos, Alberto Gonzalo, Jesús Arauzo,* and José Luis Sánchez

Cite This: *Energy Fuels* 2021, 35, 17149–17166

Read Online

ACCESS |

Metrics & More

Article Recommendations

Supporting Information

ABSTRACT: The present work summarizes the results of an experimental study focused on producing antioxidant additives for biofuels from argan shell lignin. The generation of this waste has noticeably increased in specific regions of Morocco as a result of the upward trend in the production of argan oil. Lignin extracted from argan shells via a semi-chemical pulping process was depolymerized under hydrothermal conditions in a stirred autoclave reactor at a temperature range of 250–350 °C. Lignin conversion to phenolic compounds was conducted in subcritical water together with different reaction medium (H₂, CO₂, and HCOOH). The organic fraction in the aqueous liquid product was extracted and blended with biodiesel at a dosage of 1 wt % to evaluate its antioxidant potential. According to the obtained results, the biodiesel oxidation stability time was drastically improved up to 400%. The depolymerization temperature was observed as a critical factor in the antioxidant potential of the additives, showing a maximum value at 300 °C, regardless of the reaction medium. An extensive characterization of the produced additives was performed. The phenolic monomers present in the produced additives were identified using gas chromatography–mass spectrometry, finding a notable presence of catechol, especially in the additives obtained at 300 °C, which led to the best results of biodiesel oxidation stability. Gel permeation chromatography analyses of the additives also showed a well dissolution of relatively big molecules (up to 7000 Da) in biodiesel. More efforts are required to verify the actual antioxidant potential of these types of molecules.



1. INTRODUCTION

Lignin is considered one of the most abundant biopolymers in the world (up to 40% of the dried weight in some types of lignocellulosic biomass^{1–3}). Lignin is an amorphous polymer with a complex structure that consists principally of three different monomer units: *p*-coumaryl alcohol (H), coniferyl alcohol (G), and sinapyl alcohol (S),^{2–4} linked together with condensed linkages, such as 5–5, β – β , β –5, and β –1, and/or ether linkages, such as α –O–4, 5–O–4, and β –O–4.^{5–7} The proper cleavage of these chemical bonds (depolymerization) may result in bio-based aromatic chemicals with an important additive value.

In the industrial processes, lignin can be extracted from the lignocellulosic biomass by classical chemical methods (kraft and sulfite processes) and semi-chemical methods (organosolv and soda processes), in addition to the new promising methods, such as pretreatments using ammonia⁸ or imidazole.⁹ However, as a result of its complicated structure, the extraction of an unaltered state of the native lignin is still not yet possible.⁴ A semi-chemical pulping process using soda has been a historically typical process in the production of pulp and paper from non-wood materials, such as some crops

(*Miscanthus* and kenaf) or agricultural residues (straw and bagasse).¹⁰ This process entails separating pulp with a high cellulose content from the original lignocellulosic material, leaving behind a black liquor, rich in lignin content, as a problematic byproduct to be managed.^{10,11}

Lignin conversion could be considered a potential alternative to the petrochemical industry, especially for fuel and chemical production.⁴ For its chemical valorization, lignin fragmentation can be implemented via various technologies, such as biological depolymerization, homogeneous and heterogeneous catalysis, and thermochemical treatments.¹² Generally, the main depolymerization products in thermochemical treatments are a gas stream (mainly CO₂), small organic compounds, up to 10 wt % phenolic monomers, and between 45 and 70 wt % oligomers.¹³

Special Issue: 2021 Pioneers in Energy Research:
Javier Bilbao

Received: June 2, 2021

Revised: August 5, 2021

Published: September 3, 2021



Among thermochemical treatments, hydrothermal processes are defined as chemical and physical transformations at a high pressure¹⁴ and moderate temperature (200–400 °C)¹⁵ in an aqueous solution. These processes are considered as an effective and environmentally friendly technology for the chemical valorization of lignocellulosic biomass,^{14–17} with the conveniences of a high conversion rate and short holding time.¹⁵ Several studies were dedicated to lignin fragmentation by hydrothermal treatment for chemical production.^{18,19} During this treatment, the oxygen content in the organic material can decrease from 40 to 15% through its release in the form of CO₂, H₂O, and CO.²⁰ Additionally, many reactions occur during the hydrothermal process, such as demethoxylation, alkylation, condensation, and fracture of ether and carbon–carbon bonds.^{15,21} With regard to the reaction medium, some works were focused on the performance of H₂ and hydrogen donors (such as formic acid and alcohols) on the stability of the free radicals formed during the hydrothermal depolymerization of lignin²² and its effectivity in increasing the yield of depolymerized lignin,^{7,23} halting repolymerization reactions and promoting demethoxylation.²⁴ Other gaseous reaction medium have been studied, such as CO₂,¹⁵ whose incorporation in the aqueous solution leads to carbonic acid formation, which enhanced the quality of the resulting substrates during enzymatic hydrolysis reactions.²⁵ Furthermore, other studies were focused on the effect of base catalysts [such as Ca(OH)₂, K₂CO₃, LiOH, KOH, and NaOH] on lignin depolymerization.^{26–28} This reaction medium prevents coke formation and favors the monomer and dimer production. The type of base catalyst used affects the nature of the phenolic products obtained and the organic compound yields.²⁹ According to Toledano et al., NaOH was considered as the best option to catalyze the hydrothermal depolymerization of lignin.³⁰

The lignin-derived chemical products from hydrothermal depolymerization are mainly based on phenolic compounds. In general, phenolic compounds as a whole are usually considered to have good antioxidant properties.³¹ In this field, some research works have already tested the production of antioxidants from renewable phenolic sources destined more specifically to improve the oxidation stability of biodiesel.^{5,21}

Biodiesel is an environmentally friendly fuel composed of fatty acid esters, usually synthesized through triglyceride transesterification with short-chain alcohols.³² Biodiesel can replace fossil diesel in conventional engines (decreasing the unburned carbon monoxide and smoke emissions by 30 and 50%, respectively³³) while keeping in mind essential issues related to the low storage stability of biodegradable fuels. Biodiesel is less resistant to oxidative degradation as a result of the instability caused by the unsaturation of fatty acid chains.³⁴ Its oxidation process begins by forming a peroxy radical (from a fatty acid radical in the presence of O₂). Then, this unstable radical starts the self-sustaining chain reaction, abstracting the most reactive hydrogen atoms. To avert this problem, synthetic antioxidants are usually incorporated into the biofuel with the role of interrupting the subsequent chain reaction of peroxy radicals by substituting them with new and less reactive radicals (such as phenolic radicals) to stop and retard the chain degradation.^{32,34,35} According to several studies, the use of commercial antioxidants, such as butylated hydroxytoluene (BHT), *tert*-butylhydroxyquinone (TBHQ), and 3-*tert*-butyl-4-hydroxyanisole (BHA), shows an efficient way to improve biodiesel oxidation stability.^{36,37} However, the production of

antioxidant additives using renewable materials could be a promising alternative to fossil-based additives for biodiesel and biolubricants.^{21,35,38}

During the last years, the Thermochemical Processes Research Group (University of Zaragoza, Spain) has been focused on using different lignocellulosic feedstocks^{5,38–41} for the production of natural antioxidant additives for biodiesel. The incorporation of bio-based antioxidant additives, such as bio-oil fractions, has led to excellent biodiesel oxidation stability improvements.³⁸ The present study continues in the same investigation field by processing a non-explored agro-industrial residue: argan shells. Argan shell (AS) is a waste coming from the fruit of *Argania spinosa* (L.) Skeels. The main current interest of this fruit lies in the production of argan nut oil, an increasingly widespread cosmetic oil. The extraction of this oil leaves behind 20 tons of non-valorized waste (shells) per ton of oil produced. As far as the authors are aware, no studies about the production of chemicals from AS have been published before.

Taking into account the great social and economic impact that the valorization of agricultural wastes will take in a biorefinery concept,⁴² the present work focuses on the valorization of lignin contained in AS, which was extracted through a semi-chemical process.¹⁰ The resulting black liquor contained a high amount of lignin as well as hemicellulose and inorganic matter (in the form of ash⁴) from the chemicals used in the treatment (NaOH).⁵ The solid contained in the black liquor (from now on, ASL_f, lignin-rich fraction from argan shells) was depolymerized under hydrothermal conditions (aqueous solution) at a temperature interval between 250 and 350 °C, involving different reaction medium: formic acid (HCOOH) and H₂ and CO₂ (both gases being the decomposition products of HCOOH in hydrothermal conditions). The impact of those factors on the hydrothermal treatment performance was investigated. The lignin degradation product was tested as an antioxidant additive for biodiesel to improve its oxidative stability.

2. MATERIALS AND METHODS

2.1. Material. Argan shells were provided by a Moroccan cooperative in the region of Essaouira (southwest of Morocco, 31° 30' 47" N, 9° 46' 11" W). It was crushed and characterized. Table 1 summarizes the results of the ultimate and proximate analyses, the higher heating value (HHV), and the extractive, hemicellulose, cellulose, and lignin contents. Analytical standards and methods used in the material characterization are also detailed in Table 1. As seen, AS is a material rich in lignin (up to 34 wt %) with a low ash content (0.3 wt %) and considerable HHV (19 MJ/kg). Carbon and oxygen contents are pretty similar.

2.2. Extraction and Characterization of the Lignin Fraction. Before extraction of the lignin fraction, AS was washed to remove dust and impurities and dried at room temperature overnight. Then, lignin was extracted via a semi-chemical pulping process, in which the material was digested for 4 h in an aqueous solution of sodium hydroxide (9.5 wt % NaOH with respect to the dry weight of the material) in a batch stirred reactor of 50 L at 98 °C and atmospheric pressure.^{5,10,11} The produced black liquor was separated from the remaining shells by filtration (mesh size of 100 μm) and kept in an oven at 105 °C until obtaining a dried solid, which was maintained at such a temperature during storage to prevent rehydration. The dried lignin-rich fraction (ASL_f) was characterized in terms of the molecular weight distribution, acid-insoluble lignin content, ash content, HHV, and elemental analysis. Acid-insoluble lignin was gravimetrically quantified after precipitation of the raw solid dissolved in water.¹³ HCl (0.5 N) was added to the aqueous solution to decrease the pH to

Table 1. Ultimate and Proximate Analyses, HHV, and Chemical Composition of AS

parameter	average value (\pm standard deviation)	analytical standard/methods or equipment
Proximate Analysis (wt %, As-Received Basis)		
ash	0.30 \pm 0.01	EN 14775:2010
moisture	6.5 \pm 0.1	EN 14774-3:2010
volatile matter	75.7 \pm 0.1	EN 15148:2010
fixed carbon	17.5 \pm 0.2	by difference
Ultimate Analysis (wt %, As-Received Basis)		
C	47.5 \pm 0.2	LECO CHN628
H	6.5 \pm 0.1	LECO CHN628
N	0.177 \pm 0.003	LECO CHN628
S	<0.05	LECO CHN628-628-S add-on
O	45.5 \pm 0.2	by difference
HHV (MJ/kg)	18.98 \pm 0.02	calorific bomb IKA C2000 basic
Chemical Composition (wt %, As-Received Basis)		
extractives	0.2 \pm 0.1	Soxhlet extraction using CH ₂ Cl ₂
hemicellulose	21 \pm 1	Van Soest digestion
cellulose	35 \pm 2	Van Soest digestion
lignin	34 \pm 2	Van Soest digestion

2. The solution was heated to approximately 70 °C during 20 min and then filtered with a Büchner funnel to separate acid-insoluble lignin.

The molecular weight distribution was measured by gel permeation chromatography (GPC) using high-performance liquid chromatography (HPLC) Agilent 1200 equipment. The equipment consists of two columns (Ultrasphere 250 by Waters) and ultraviolet–visible (UV–vis) (280 and 250 nm)/refractive index (RI) detectors. The columns and detectors were maintained at 40 °C under operation. An aqueous solution (pH 12) of NaOH/methanol (1:1, by weight) with 0.1 vol % LiBr and 0.05 vol % NaN₃ was used as the mobile phase (flow rate of 0.8 mL/min). For the analysis, the solid was dissolved at a concentration of around 1 g/L. A total of 13 different polyethylene glycol standards ranging from 106 to 100 900 Da were used for calibration (more information is shown in Figure S1 of the Supporting Information). The results of GPC were expressed in terms of the average molecular weight in number (M_n) and in weight (M_w) and polydispersity.

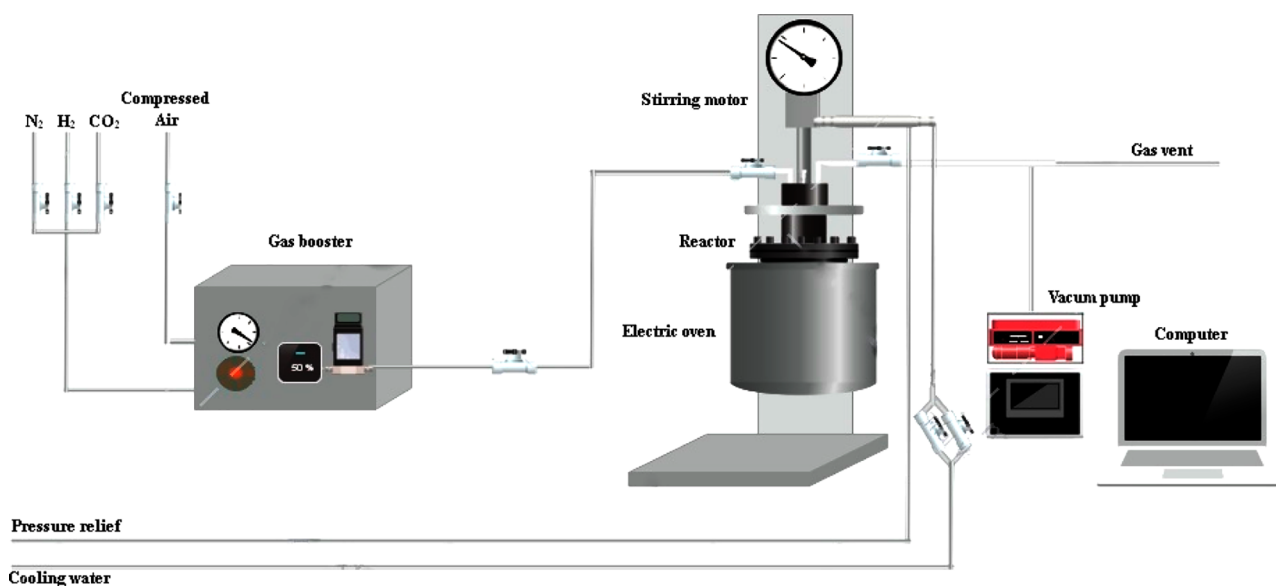
2.3. Lignin Depolymerization Experiments: Hydrothermal Treatment. The depolymerization experiments were carried out in a

500 mL Parr reactor (Parker, Inc., U.S.A.) operating in a discontinuous system (Figure 1). In a typical run, an aqueous solution of 200 g with 7 wt % ASL_f was homogeneously prepared and loaded to the reactor. Different liquid and gas medium were selected for the depolymerization process. On the one hand, HCOOH was added to the aqueous solution (under a N₂ atmosphere) as a hydrogen donor. On the other hand, H₂ and CO₂ atmospheres were also tested, aiming at evaluating their individual effect on the product distribution and antioxidant activity, because these gases are the major products of HCOOH decomposition under the experimental conditions set.⁷

In the HCOOH experiments, the selected amount (14 or 28 g, leading to a mass ratio between HCOOH and ASL_f of 1 or 2, respectively) was slowly added to the aqueous mixture before closing the reactor. The pH of the reaction mixture and the final mixture after the experiment were measured with a Thermo Orion Star A215 pH/conductivity benchtop multiparameter meter.

Once the reactor was sealed, the air was evacuated using a vacuum pump and purged with pressurized N₂ (a common step in all experiments to check leakage and remove air). Moreover, in the experiments using H₂ or CO₂, some further purges involving the pressurized reagent gas were required. After the purge stage, the reactor was finally loaded with the selected pressure of H₂ or CO₂ (25 or 50 bar) just before starting the heating. The reactor temperature was raised to the specified temperature (250, 300, or 350 °C) at a heating rate of 5 °C/min and then held constant for 1 h. The stirring was fixed at 1000 rpm throughout the experiment and also during the reactor cooling. Once the experiment had finished, the reactor was quickly cooled by moving tap water into the built-in cooling coil. The produced gas phase was collected in a gas bag and analyzed with a microgas chromatograph (Agilent 3000A).

The aqueous liquid product was recovered from the reactor, and the reactor walls and stirrer were washed with methanol, filtering both liquids together under vacuum conditions (using a pre-weighed filter paper). Methanol was used as washing solvent to ensure the recovery of the water-insoluble organic phase that remained stuck on the walls, stirrer, and cooling coil. The solid remaining in the filter was dried at 105 °C overnight and weighted to determine the yield of insoluble solid (Y_{IS}) according to eq 1. An aliquot of the filtered liquid was also dried at 105 °C (three replicates) to determine the yield of soluble solid (Y_{SS} , eq 2). Although some volatile organics can be lost during drying, the organic compounds considered of interest as an antioxidant (mainly phenolics) have vapor pressures that are low enough to be hardly affected

**Figure 1.** Hydrothermal experimental plant (Parr reactor).

$$Y_{IS} \text{ (wt \%)} = \frac{W_{IS}}{W_{ASL_f}} \times 100 \quad (1)$$

$$Y_{SS} \text{ (wt \%)} = \frac{X_{SS}W_{FL}}{W_{ASL_f}} \times 100 \quad (2)$$

where W_{IS} is the weight of the insoluble filtered solid (g), W_{ASL_f} is the weight of the dried lignin-rich fraction initially loaded in the reactor (g), W_{FL} is the weight of the total filtered liquid (aqueous reaction product + washing methanol) (g), and X_{SS} is the content of soluble solid in this liquid (wt %).

A full factorial design 2^k with two factors and two levels was established for each reaction medium (H_2 , CO_2 , and $HCOOH$) to study the influence of the temperature (250–350 °C) and the initial amount of reagent (0–50 bar of H_2 or CO_2 and 0–28 g of $HCOOH$) on the production and characteristics of the antioxidant additives. Three replicates in the central point of the factor levels (300 °C, 25 bar of H_2 or CO_2 , or 14 g of $HCOOH$) were carried out for evaluating the experimental error. In the end, a total of 17 runs were performed. Table 2 summarizes the experimental conditions tested (factors and levels).

Table 2. Experimental Design Planned for the Depolymerization Experiments

experiment number	reaction medium	T (°C)	initial gas (H_2/CO) pressure (bar)/ $HCOOH$ weight (g)
1	inert atmosphere experiments	250	0
2		350	0
3	H_2 experiments	250	50
4		350	50
5		300	25
6	CO_2 experiments	300	25
7		300	25
8		250	50
9		350	50
10		300	25
11		300	25
12		300	25
13	$HCOOH$ experiments	250	28
14		350	28
15		300	14
16		300	14
17		300	14

Some experimental data, such as the production of insoluble solid (eq 1) and soluble solid (eq 2) after ASL_f depolymerization, the C/H ratio in each solid, the additive yield (see section 2.4), the solubility of the additives in biodiesel (see section 3.4), and the performance as antioxidants for biodiesel (see section 2.5), were analyzed through analysis of variance (ANOVA) with a confidence level of 90%, and the least significant difference was calculated. Hence, the significant effects of the factors as well as their interactions were highlighted.

2.4. Additive Preparation and Characterization. An aliquot of the filtered liquid (about half of it) was extracted using twice the weight of isopropyl acetate (chosen as the extracting solvent according to a previous study, in which a large variety of solvents were evaluated⁴¹). The mixture was shaken for 10 min in a funnel and then left to decant at room temperature. The decanted aqueous phase was separated and discarded, while the organic phase (OP) was filtered using silicone-treated filter paper to remove aqueous-phase particles that remained in suspension. Three aliquots of OP (15 g each) were dried during 48 h at 50 °C to determine the concentration of extracted compounds, and from this value, the additive yield ($Y_{additive}$) was calculated according to eq 3 (from now on, the dried OP will be referred to as “additive” throughout this paper)

$$Y_{additive} \text{ (wt \%)} = \frac{X_{OP}W_{OP}W_{FL}}{W_{EL}W_{ASL_f} \text{ (ash-free)}} \times 100 \quad (3)$$

where X_{OP} is the concentration (wt %) of the lignin-derived compounds in the OP, W_{OP} is the weight (g) of OP obtained after the extraction, and W_{EL} is the weight (g) of the aqueous liquid subjected to extraction. Here, W_{ASL_f} is expressed on an ash-free basis involving only the organic fraction present in the raw material.

For chemical characterization, the additives were redissolved in methanol and analyzed by gas chromatography (GC) with an Agilent 7890A gas chromatograph equipped with a flame ionization detector (FID) and combined with an Agilent 5975C mass selective detector (MSD) (operating parameters were detailed in Table S1 of the Supporting Information). For the calibration of the FID signal, eight standard solutions, including the most abundant phenolic components in the samples (guaiacol, creosol, 2,4,6-trimethylphenol, phenol, 4-ethylguaiacol, 2,5-dimethylphenol, *p*-creosol, eugenol, 4-ethylphenol, 2,6-dimethoxyphenol, 3-methoxycatechol, 4-allyl-2,6-dimethoxyphenol, vanillin, apocynin, guaiacylacetone, catechol, homovanillyl alcohol, and hydroquinone), were prepared using dichloromethane/methanol (1:1, by volume) as the eluent. The concentration of each compound in the standard solutions ranged between 50 and 3000 $\mu\text{g/mL}$. Moreover, the concentrations of the compounds that were identified by mass spectrometry (MS) but not included in the standards was calculated from the response factor of the most similar standards used, applying to it a correction factor according to a methodology based on the effective carbon number (ECN).^{25,43,44}

The structural composition of the additives was also investigated using a Fourier transform infrared (FTIR) spectrometer, Agilent Cary 630 FTIR.

For further characterization, the molecular weight distribution of the additives as well as their biodiesel-insoluble fractions (see section 2.5), was measured by GPC following the same procedure detailed for the raw lignin.

2.5. Blend of Biodiesel and Additives and Measurement of Oxidation Stability. The biodiesel used in this study was synthesized in the laboratory using sunflower oil and methanol as reagents (molar ratio of methanol/oil of 6:1) and potassium hydroxide as the catalyst (1% of oil mass). The biodiesel production process has been described in greater detail elsewhere.^{5,38,39,41}

To start the procedure of incorporating the additives to biodiesel, a portion of the OP extracted was evaporated in a rotary evaporator at 60 °C and vacuum conditions (10 mbar absolute pressure). The remaining dried solid (i.e., the additive itself) was weighed; therefore, the appropriate amount of neat biodiesel could be added to the same flask, adjusting it to an initial additive dosage of 1 wt %. To enhance the additive dissolution in the biodiesel, methanol was used as a co-solvent (with a mass ratio of methanol/biodiesel of 1:1) and the mixture was sonicated for several minutes in an ultrasound bath. Then, methanol was removed in a rotary evaporator. The final mixture of biodiesel and additive was centrifuged to separate the additive-insoluble fraction. The homogeneous mixture of doped biodiesel was recovered from the upper part of the centrifugation tube, while the insoluble fraction remaining at the bottom was thoroughly washed with hexane (with sonication) to remove biodiesel traces. Then, the washed solid was dried overnight at 50 °C and weighed to determine the fraction of insoluble additive and, by difference, the dosage of additive that was really dissolved in biodiesel. As commented before, GPC analyses were conducted on these insoluble fractions of the additive.

The oxidation stability of both neat and doped biodiesel samples was measured according to EN 16091 and ASTM D7545 methods through a PetroOXY tester device (Petrotest Instruments GmbH & Co.). The oxidation stability was measured as the time required by the biodiesel samples (5 mL) to reduce by 10% the oxygen pressure initially established in the measurement vessel.

Figure 2 summarizes all of the steps in the experimental procedure developed in this work, from the initial stage of lignin extraction from AS to the last step of measurement of the oxidation stability of biodiesel after incorporating the antioxidant additives.

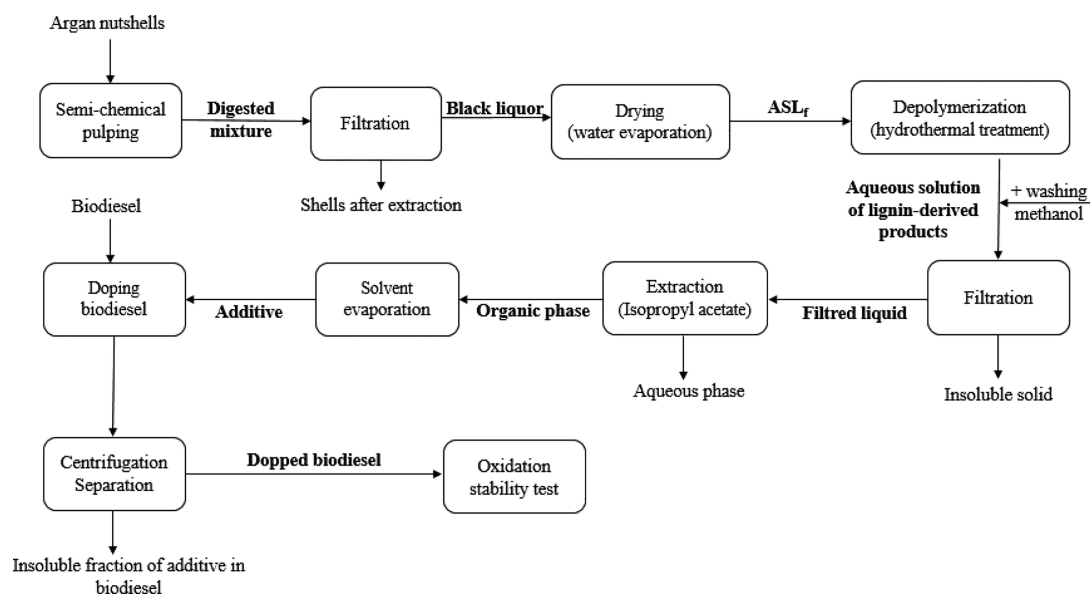


Figure 2. Experimental steps: lignin extraction, lignin depolymerization, additive preparation, and mixture with biodiesel and oxidation stability tests.

3. RESULTS AND DISCUSSION

3.1. Characterization Results of the Lignin-Rich Fraction Extracted from Argan Shells. The yield of the lignin fraction extracted from AS by the semi-chemical pulping treatment was up to 22% with respect to the initial lignin contained in the raw material (ash-free basis). As commented before, the content of acid-insoluble lignin in this extracted fraction was determined gravimetrically, accounting for 43 wt % of the organic fraction in the solid (ash-free basis). [Table 3](#)

Table 3. Characterization of the Lignin-Rich Fraction Extracted from AS

parameter	average value
C (wt %)	75.2 ± 0.1
H (wt %)	7.78 ± 0.04
N (wt %)	0.58 ± 0.02
S (wt %)	<0.05
O (wt %) ^a	16.4 ± 0.2
HHV (MJ/kg)	10.33 ± 0.04

^aBy difference.

shows other characterization results of the extracted and dried ASL_f (ash-free basis). The ash content in ASL_f was much higher (up to 60 wt %) than the initial ash content in AS (0.3%). This high ash content could be explained by the presence of much of NaOH used in the pulping treatment,^{4,5} which will benefit the subsequent depolymerization process, because NaOH could be considered a base catalyst in the hydrothermal process.¹⁹ According to Toledano et al.,²⁹ NaOH is a suitable base catalyst for lignin depolymerization in terms of conversion and fractionation to phenolic monomers.

With regard to the molecular weight distribution of ASL_f, M_w was found to be 37 900 Da, M_n was 24 200 Da, and polydispersity was 1.6.

3.2. Product Distribution in the Hydrothermal Treatment. During depolymerization, ASL_f has been mainly converted to water-soluble and -insoluble solid compounds

(or liquids in the case of some specific soluble compounds). Only a minimal amount of gases was generated in the process. Mass balance (without including the few produced gases) was closed fairly well (between 86 and 100.8%). With regard to the produced gas, [Figure S2](#) of the Supporting Information shows the residual gas pressure in the reactor after cooling (at 20 °C). As shown, at the inert atmosphere reaction medium, only up to 0.4 bar of gas was generated after the experiment at 250 °C, a value that increased to 2 bar at 350 °C. In both cases, the gas product was essentially composed of CO₂ and traces of H₂. In the case of the H₂ experiments conducted at 350 and 300 °C, the amount of residual gas was lower than the initial pressure loaded in the reactor, which points to a net consumption of H₂ during the reaction. However, a slight increase in the total amount of gas was detected at 250 °C as a consequence of higher CO₂ production, thus hiding H₂ consumption. In the case of CO₂ experiments, generation of residual gas (around 5 bar) was only observed when initially loading the highest pressure of CO₂ in the reactor (at both 250 and 350 °C). As expected, the composition of this residual gas was essentially CO₂ (between 90 and 98 vol %). Lastly, a drastic increase in pressure was observed in HCOOH experiments as a result of the formic acid decomposition into H₂, CO₂, and CO at this temperature range according to two possible pathways ([reactions R1 and R2](#)).⁴⁵



[Table S2](#) of the Supporting Information shows the maximal pressures reached during each experiment. As shown, these pressures were varied from one reaction medium to other and, obviously, depending upon the temperature.

With regard to other products formed in the hydrothermal treatment of ASL_f, the joint yield of soluble and insoluble solids ($Y_{SS} + Y_{IS}$) (shown in [Figure S3](#) of the Supporting Information) ranged between 88 and 96% in most experiments, except on some of those experiments carried out with HCOOH, in which this joint yield exceeded 100%, reaching

Table 4. Product Distribution, C/H Ratio in the Solids, and Additive Yields

reaction medium	T (°C)	initial gas (H ₂ /CO) pressure (bar)/HCOOH weight (g)	Y _{IS} (wt %)	Y _{SS} (wt %)	C/H ratio		Y _{additive} (wt %)
					C/H _(IS)	C/H _(SS)	
inert atmosphere	250	0	0.86	93.58	9.2 ± 0.1	8.0 ± 0.6	6.42
	350	0	2.01	86.18	15.1 ± 0.1	9.1 ± 0.3	21.29
H ₂	250	50	0.81	92.70	9.8 ± 0.1	7.6 ± 0.1	13.18
	350	50	1.38	86.88	12.9 ± 0.1	7.4 ± 0.4	20.50
	300	25	1.04	92.27	12.13 ± 0.04	7.5 ± 0.3	13.49
	300	25	0.80	95.17	12.3 ± 0.05	6.89 ± 0.02	19.13
	300	25	0.76	92.20	12.3 ± 0.2	7.9 ± 0.1	17.94
CO ₂	250	50	3.90	92.10	13.4 ± 0.2	8.5 ± 0.1	18.48
	350	50	3.92	88.17	16.3 ± 0.6	9.4 ± 0.4	24.38
	300	25	3.26	89.24	16.0 ± 0.2	8.36 ± 0.01	14.49
	300	25	3.32	89.44	15.8 ± 1.4	9.3 ± 0.2	17.54
	300	25	3.58	91.78	16.1 ± 0.1	8.7 ± 0.3	17.09
HCOOH	250	28	2.98	102.60	10.4 ± 0.1	6.8 ± 0.3	38.80
	350	28	2.46	90.63	10.6 ± 0.2	7.1 ± 0.2	28.08
	300	14	2.72	112.16	11.3 ± 0.5	4.6 ± 0.2	18.24
	300	14	3.36	109.60	10.9 ± 0.2	4.5 ± 0.1	24.11
	300	14	3.58	99.24	11.2 ± 0.1	5.828 ± 0.001	21.06

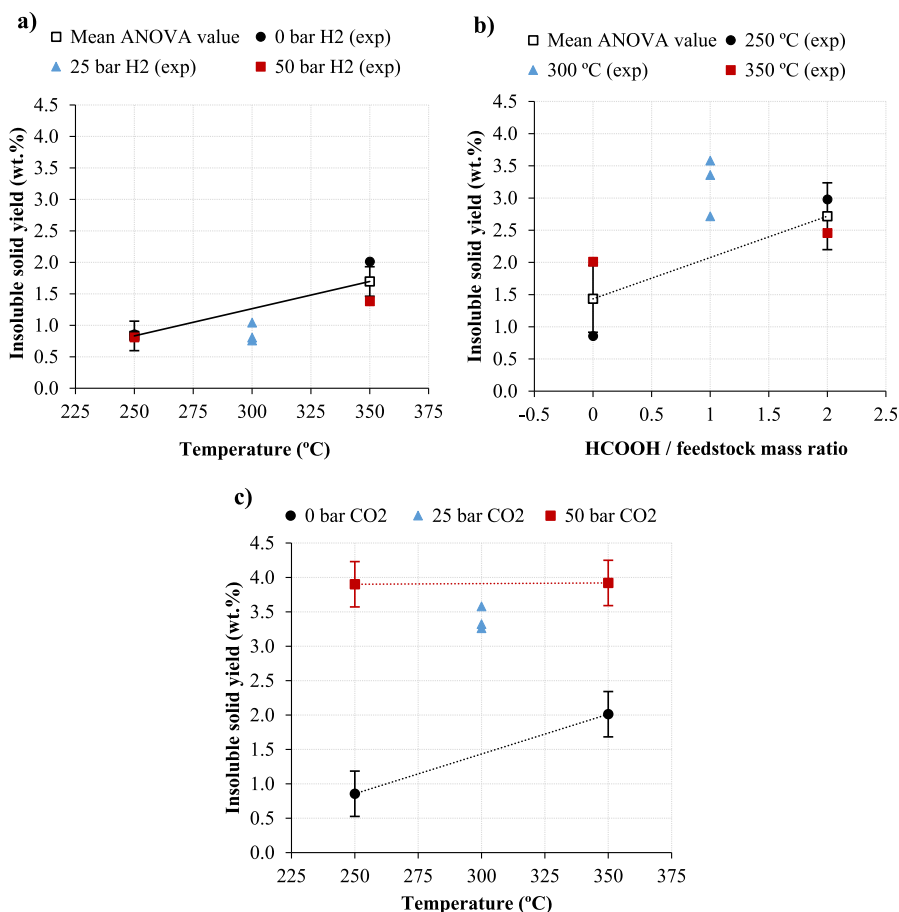


Figure 3. Effect of the temperature and reagent amount used in the depolymerization experiments on the yield of insoluble filtered solid (wt %): (a) H₂ experiments, (b) HCOOH experiments, and (c) CO₂ experiments.

values even up to 110%. Such high values could be due to the precipitation of sodium bicarbonate (NaHCO₃), which may be formed in the reaction between dissociated CO₂ from HCOOH decomposition and Na⁺ from NaOH present in ASL_F. It should be highlighted that the initial pH of the reactional mixture decreased from 10.5 to around 3 with the

addition of HCOOH, which indicates neutralization of NaOH by HCOOH before heating the reaction system.

The influence of the operational factors on the production of soluble and insoluble solids is detailed more specifically below.

3.2.1. Insoluble Solid Yield. Among other results, Table 4 shows the yield of insoluble solid obtained under the different

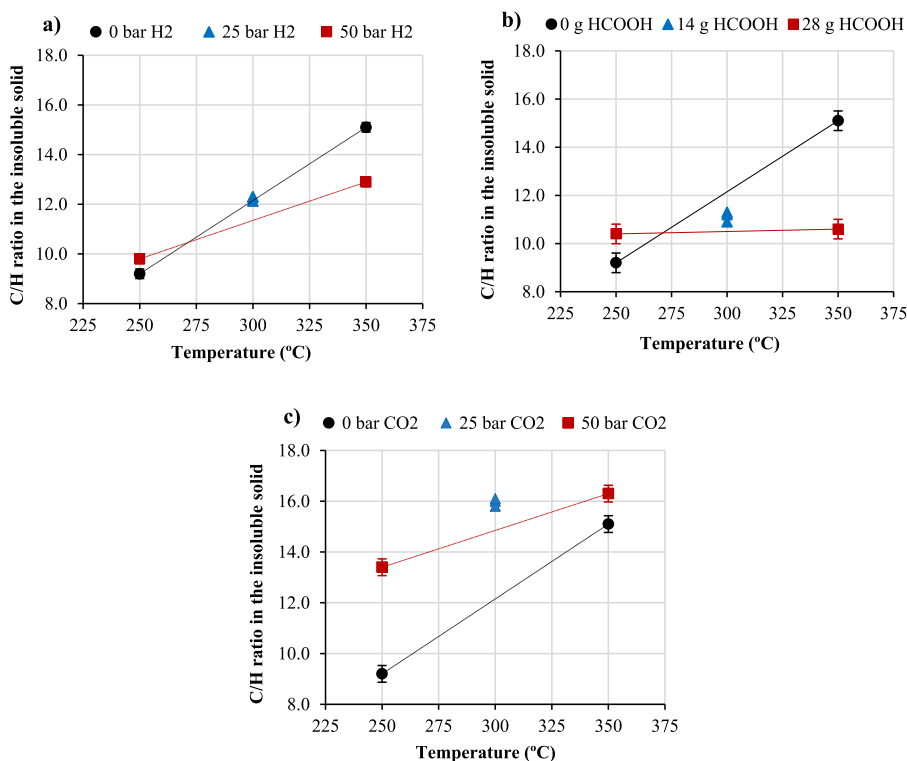


Figure 4. Effect of the temperature and reagent amount used in the depolymerization experiments on the C/H ratio of the insoluble filtered solid (wt %): (a) H₂ experiments, (b) HCOOH experiments, and (c) CO₂ experiments.

operational conditions. For a better interpretation of the results, Figure 3 plots the ANOVA statistical analysis of this response parameter (error bars correspond to the least significant difference at a confidence level of 90%). Both the experimental data (denoted in the figures as filled symbols and named) and the theoretical values resulting from the one-way ANOVA (denoted in the figures as “mean ANOVA value”) have been represented in the figures, thus giving a first approach of the good or bad fitting of the models in the high and low levels of the experimental design. If the mean ANOVA value does not appear in a figure, it means that experimental and theoretical values are just the same.

As seen in Figure 3a, the depolymerization temperature showed a significant positive effect on the production of insoluble solid in the case of operating under an inert atmosphere or with H₂ as a reaction medium. This increase in the insoluble solid yield was interpreted according to many studies by the condensation or repolymerization reactions that could occur at temperatures higher than 300 °C.^{7,46,47} The repolymerization/condensation reaction has been reported by several studies and explicated as the reaction between unstable lignin fragments and original lignin.^{29,48} According to Li et al.,⁴⁹ the key point of these reactions is the carbenium ion generated at the α -carbon atom. After the ether bond cleavage, this ion can be attacked by an adjacent aromatic ring forming a stable carbon–carbon bond that increases the molecular weight^{28,29} and could change the molecular structure. Contrary to what was expected, the presence of H₂ did not show a significant impact on the insoluble solid yield with respect to the experiments carried out under the initial inert atmosphere (Figure 3a). According to various studies in the literature, some H-donating reaction medium (in the presence of alcohols or acetone) have been proven to reduce char

formation.^{18,50} However, this effect was not observed in the present work. In fact, the addition of HCOOH as a H donor to the reaction medium even showed the opposite effect, because the production of the insoluble yield was augmented in comparison to the inert atmosphere results (Figure 3b). That seems to be correlated with the generation of CO₂ from HCOOH, as in the case of CO₂ experiments (Figure 3c). The presence of CO₂ had a remarkable effect on the increase of the insoluble solid yield, which was maintained stable (around 4%) throughout all of the temperature range (and $P_{\text{CO}_2} = 50$ bar). A significant interaction between both factors has been observed: the temperature showed a positive effect on the production of the insoluble yield in the absence of CO₂, while that effect disappeared by initially feeding CO₂ or HCOOH.

In short, the most unfavorable operating conditions from the point of view of the generation of such an insoluble solid, which is an undesirable byproduct for the purpose of the process, involves high amounts of CO₂ in the reaction medium. To minimize its production, the optimal working conditions would be the most moderate reaction temperature (250 °C) and either inert or H₂ atmospheres (Y_{IS} of around 0.8 wt %).

The C/H ratio in both the insoluble and soluble solids was calculated using the elemental analysis data summarized in Table S3 of the Supporting Information. These data are included in Table 4. The ANOVA of the C/H ratio in the insoluble solid is shown in Figure 4. The temperature, the reaction medium, and the interaction between them had a significant effect on this C/H ratio. The presence of CO₂ had a positive effect on the C/H ratio in the entire temperature interval, while the presence of H₂ or HCOOH contributed to increase the fraction of H in the solid formed at the highest temperature.

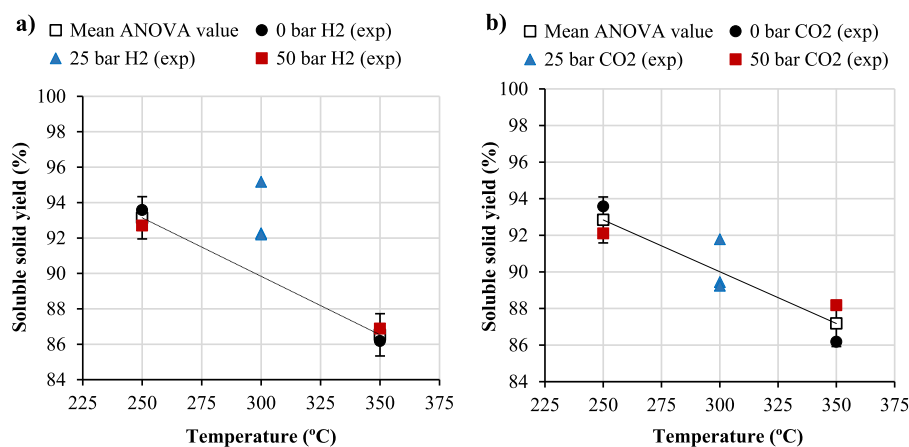


Figure 5. Effect of the temperature and reagent amount used in the depolymerization experiments on the yield of soluble filtered solid (wt %): (a) H₂ experiments and (b) CO₂ experiments.

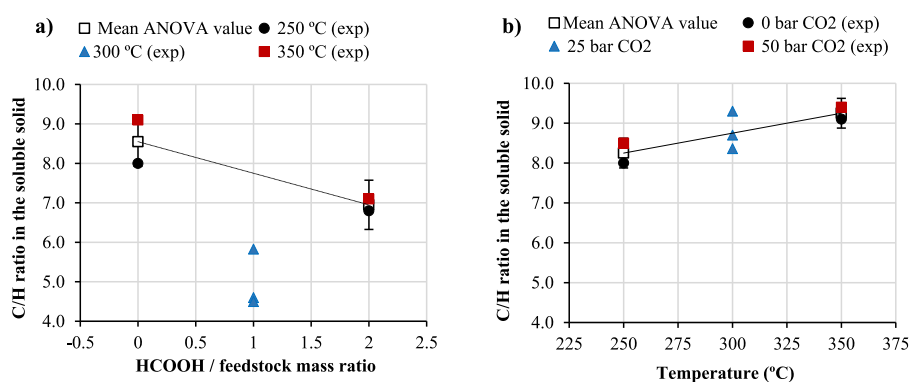


Figure 6. Effect of the temperature and reagent amount used in the depolymerization experiments on the C/H ratio of soluble filtered solid (wt %): (a) HCOOH experiments and (b) CO₂ experiments.

3.2.2. Soluble Solid Yield. Figure 5 shows the ANOVA of the results obtained for the yield of soluble solid produced under the different reaction medium and temperatures (Table 4). The operational factors did not affect this response parameter in HCOOH experiments (no significant effect was detected). However, according to ANOVA, the treatment temperature had an apparent negative effect on the yields of soluble solid in the presence of H₂ and CO₂, while the initial pressure of gas loaded in the reactor did not show a significant effect on either of the two reaction medium. In the case of H₂ experiments, data did not fit a linear model (significant curvature), which may be related to the temperature profile, because the amount of H₂ present in the reaction medium was found to have a non-significant effect.

It should be noted that the distribution of the solid product into the soluble or insoluble fractions was really affected by the amount of methanol used in washing the reactor and the filtered solid, because methanol plays a co-solvent role and can enhance the dissolution of some water-insoluble compounds in the aqueous methanol phase. Therefore, the amount of methanol used for washing was similar in all of the experiments.

Figure 6 shows the ANOVA of the C/H ratio in the soluble solid. No significant effect of the operational factors was detected for this response parameter in H₂ experiments. In the presence of CO₂ (Figure 6b), a slightly positive and linear effect of the temperature was observed. In the case of

HCOOH experiments (Figure 6a), data showed a non-linear model (with significant curvature).

As shown in Table S4 of the Supporting Information, the fraction of these three elements yielding soluble compounds was found to be significantly higher than that producing insoluble compounds, regardless of the experimental conditions.

3.3. Additive Yields. Table 4 reports the yields of the produced additives under the different experimental conditions. The ANOVA of the results (Figure 7) shows that both the temperature and reaction medium had a significant effect on the additive yield obtained as a whole. A linear trend in the additive production relative to the temperature was observed, with a clear positive effect in the case of H₂ experiments and CO₂ experiments and a slight negative effect in the case of HCOOH experiments. With regard to the influence of each reaction medium, no significant effect of H₂ presence has been found. In contrast, in the presence of CO₂, a positive effect of the initial pressure of gas was observed in the entire temperature interval, which means that the additive production when 50 bar of CO₂ was initially fed in the reactor was greater than that obtained in the initial inert atmosphere. The same occurred in the case of HCOOH experiments, although this drastic positive effect was only reported at the lowest temperature (250 °C), because the interaction between both factors was found to be significant in this reaction medium. The use of HCOOH was the most favorable reagent from the point of view of maximizing the production of additives,

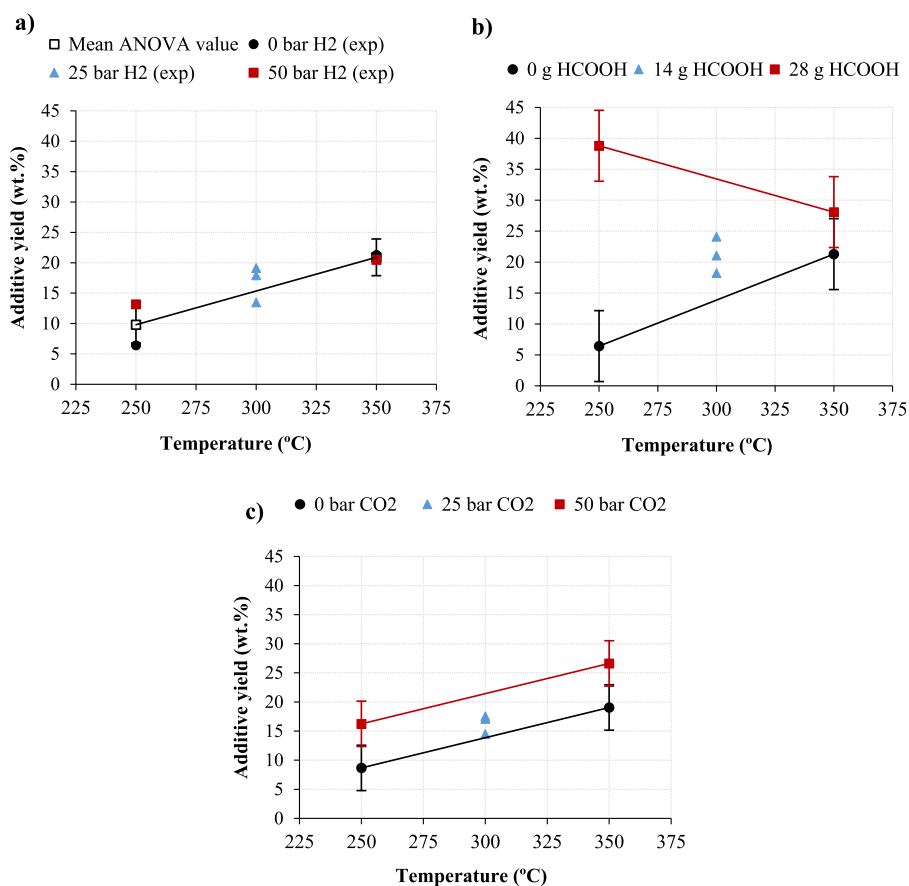


Figure 7. Effect of the temperature and reagent amount used in the depolymerization experiments on the additive yield (wt %): (a) H₂ experiments, (b) HCOOH experiments, and (c) CO₂ experiments.

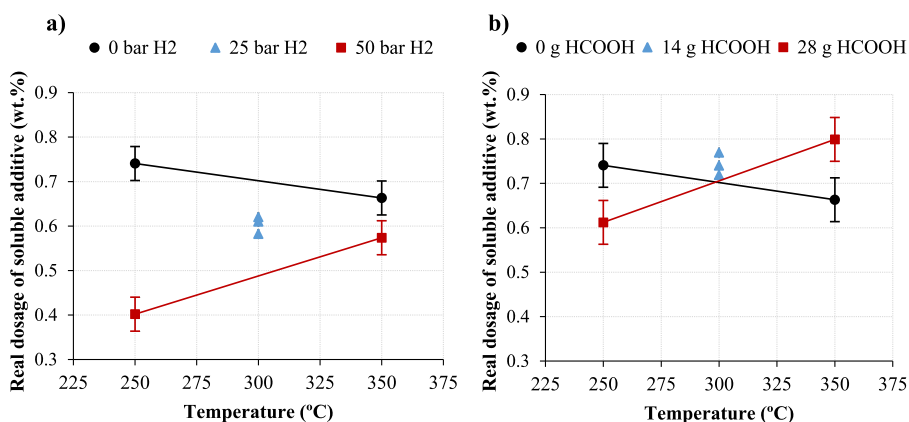


Figure 8. Effect of the temperature and amount of H₂ and HCOOH used in the depolymerization experiments on the additive solubility in biodiesel (wt %): (a) H₂ experiments and (b) HCOOH experiments.

especially operating at 250 °C and with an initial amount of 28 g of HCOOH (HCOOH/ASL_f mass ratio of 2), which led to a maximum additive yield of around 39 wt %.

3.4. Additive Solubility in Biodiesel. The dried additives were individually mixed with biodiesel at an initial dosage of 1 wt %. However, after centrifugation, it could be observed that the entire additive was not homogeneously dissolved in biodiesel. The real dosage of soluble additive was determined after centrifugation and separation of the insoluble fraction according to eq 4

$$\text{real dosage of soluble additive (\%)} = \frac{W_{\text{initial additive}} - W_{\text{insoluble additive}}}{W_{\text{biodiesel}} + (W_{\text{initial additive}} - W_{\text{insoluble additive}})} \times 100 \quad (4)$$

where $W_{\text{initial additive}}$ is the weight (g) of the additive initially added to biodiesel, $W_{\text{insoluble additive}}$ is the weight (g) of the insoluble additive quantified after centrifugation, hexane washing, and drying, and $W_{\text{biodiesel}}$ is the weight (g) of neat biodiesel used for the mixture.

Table 5. Concentration of Monomeric Phenolic Compounds in the Additives Produced at Different Conditions

compound	concentration in the dried additives (mg/g)																	
	inert atmosphere experiments			H ₂ experiments			CO ₂ experiments			HCOOH experiments								
	250 °C	350 °C	250 °C, 50 bar	350 °C, 50 bar	300 °C, 25 bar	250 °C, 50 bar	350 °C, 50 bar	300 °C, 25 bar	250 °C, 28 g	350 °C, 28 g	300 °C, 14 g							
guaiacol	18	1	24	1	2	3	3	8	0.3	11	4	2	0.2	6	1	1	3	
2,6-dimethylphenol			0.5	1	0.5	0.3	0.5						0.1	0.4	0.3			
creosol	2	0.3	2	1	1	1	1	0.3	0.2	3	1	1	0.1	1	0.5	0.4	1	
1,2,3-trimethoxybenzene	2	0.1	2			0.2	0.2	0.3	0.2				0.3					
2,4,6-trimethylphenol				0.5					0.1				0.2	0.2	0.5			
phenol	2	0.4	3	6	1	1	2	1	1	5	1	1	1	3	1	0.5	1	
4-ethylguaiacol	2	0.1	2		0.4	0.5	0.4	1	0.03	2	1	0.3		2	1	1	2	
3-ethylphenol	1			0.5					0.1									
<i>p</i> -cresol	3			3	0.2	0.4	0.3		1	1	0.3	0.1	1	0.4		0.1	0.3	
2-methoxy-4-propylphenol								0.2		1		0.3	0.3	2	1	1	1	
4-ethylphenol			0.2	1	0.5	0.4	0.3	0.1	0.5	1		0.2	1	1	0.2	0.2	0.4	
3,4-dimethylphenol				0.5				0.2	1	1	1	0.2	0.3					
syringol	148	0.2	71	0.4	1	1	1	27	1	3	2	1	5	3	6	4	9	
3,5-dimethoxy-4-hydroxytoluene	39	0.1	20		0.5	0.3	0.4	2		1	1	1	1	1	0.5	0.3	1	
1,2,3-trimethoxy-5-methylbenzene	16	0.4	8		0.3	1	0.2	3		1	0.5	0.2		4				
<i>m</i> -guaiacol	1	1	0.4			0.3		0.1	0.3									
2-allyl-4-methylphenol													0.3					
vanillin	4		1	1	0.5	1	1	0.3	0.4			0.5	0.2					
4-butyl-1,2-dimethoxybenzene	4		2	1	0.3	0.3		1	1				0.5					
apocynin	8		4		2	1	2	1	1	1	2	0.6		0.5				
guaiaacylacetone	8	0.5	5					4	0.4			1	0.4	1.5	2	1.2		
catechol	35		18	30	51	64	36	16		54	32	19		11	15	12	24	
3-methylcatechol					6	13				12	9		3				13	
homovanillyl alcohol	2	0.2						1						9	5	3	4	
4-ethylcatechol														4	4	3	6	
4-hydroxy-3-methoxybenzenepropanol			9	1	1	0.5	0.3	5		1	2	1		4	3	2	3	
4-hydroxybenzeneeethanol								1					0.3	1	4	3	3	
desaspidinol	4		3											4				
hydroquinone										1	1	0.2		2	5	3	6	

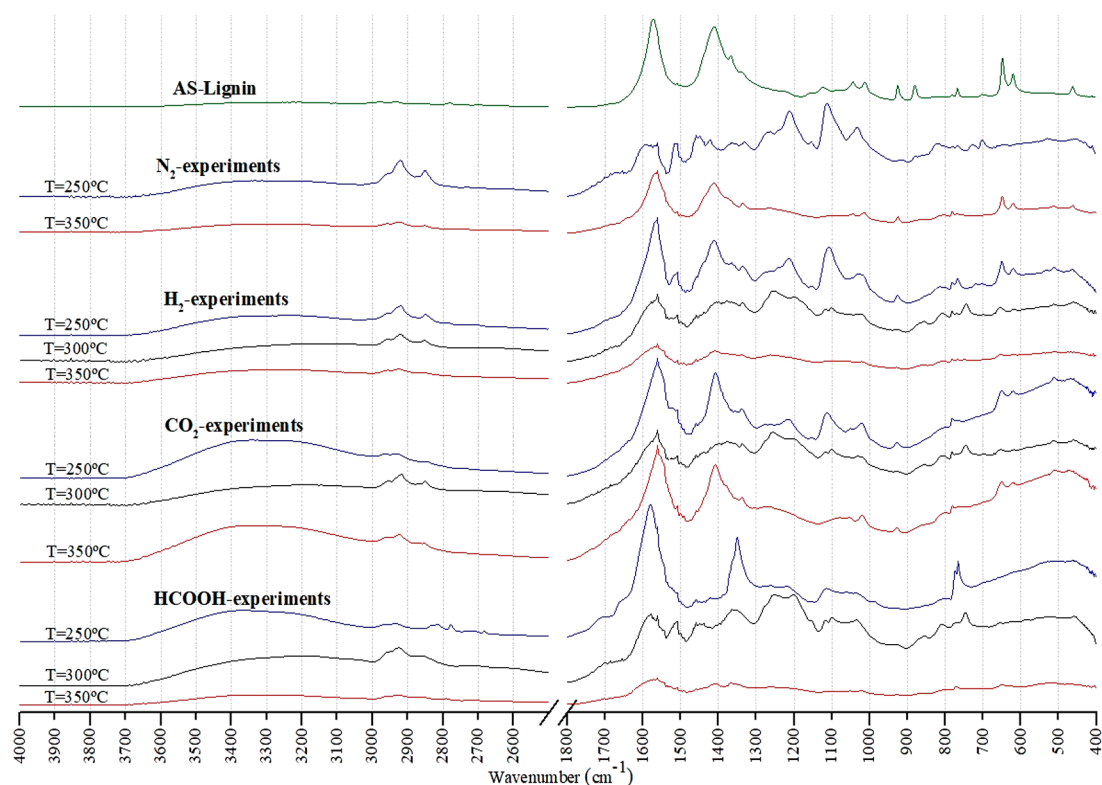


Figure 9. FTIR spectra of the additives prepared at different operational conditions and ASL_r.

Figure 8 shows the effect of both the temperature and amount of H₂ or HCOOH used in the depolymerization experiments on the additive solubility in biodiesel. As shown, at the lowest temperature (250 °C), the presence of H₂ (50 bar initially) led to a much less soluble additive than that obtained in the case of operating with an inert atmosphere. This difference in the solubility of both additives was considerably reduced at 350 °C. Moreover, the solubility of the additives produced under an inert atmosphere was damaged with the temperature, while it improved under H₂ medium (significant interaction between both factors). The same trend was observed for solubility of the additives obtained under HCOOH medium, although these data were noticeably better than those obtained for H₂ medium. The most soluble additive (real additive dosage incorporated to biodiesel of 0.8 wt %) was obtained under HCOOH medium at 350 °C. Concerning the CO₂ presence during the additive production and according to ANOVA, the additive solubility was not significantly affected by the operational factors, ranging between 0.52 and 0.67 wt %, irrespective of the temperature and initial pressure of CO₂ loaded.

3.5. Additive Characterization. **3.5.1. GC–FID–MS Analysis of the Additives.** The GC–FID–MS analysis revealed the presence of a wide variety of monomeric phenolic compounds as well as acetic acid, aldehydes, and furans. Table 5 shows the concentration of the monomeric phenolic compounds expressed as milligrams per gram of the dried additive. As shown, some of the major phenolic compounds identified were phenol, guaiacol, syringol, and catechol as well as their alkyl- and methoxy-substituted derivatives. Catechol was identified as the predominant compound at 300 °C, regardless of the reaction medium, while syringol was the main phenolic product at 250 °C, especially in the case of using an inert medium. In general (except for the HCOOH medium), the

increase in the depolymerization temperature led to a reduction in the concentration of syringol and guaiacol, while catechol and catechol derivatives increased their concentrations. However, using HCOOH as a reaction medium, only traces of guaiacol were detected in the additive produced at 250 °C, which increased proportionally with the temperature, while no apparent effect of the temperature was detected on the syringol concentration. In this reaction medium (HCOOH), a wider variety of phenolic monomers was observed in the produced additives, especially at high temperatures. In addition to catechol and catechol derivatives, the presence of other monomers, such as hydroquinone, 4-hydroxybenzeneethanol, 4-hydroxy-3-methoxybenzeneethanol, and homovanillyl alcohol, has been found at a level comparable to guaiacol or syringol.

According to several studies in the literature,^{29,30,48} at severe conditions of temperature (at least 300 °C) and in the presence of base catalysts, both guaiacol and syringol directly coming from lignin fragmentation are intermediate products that could undergo demethylation, demethoxylation, and dealkylation reactions to produce advantageous products, such as phenol, catechol, catechol derivatives, and creosol. This finding is in agreement with the observations found in this work for inert, H₂, and CO₂ atmospheres, because ASL_r contains an important amount of NaOH used for the extraction of lignin from AS. Trends were not so clear for the HCOOH medium, which could be due to the acidic character of this reactional mixture. As shown in Table S5 of the Supporting Information, an alkaline reaction medium was maintained throughout the experiments in the cases of an initial inert atmosphere and H₂ medium, while in the case of the CO₂ experiment, the pH of the reactional mixture was neutralized. However, different pH values were measured after the experiments in the case of HCOOH medium: 4.8, 6.3, and

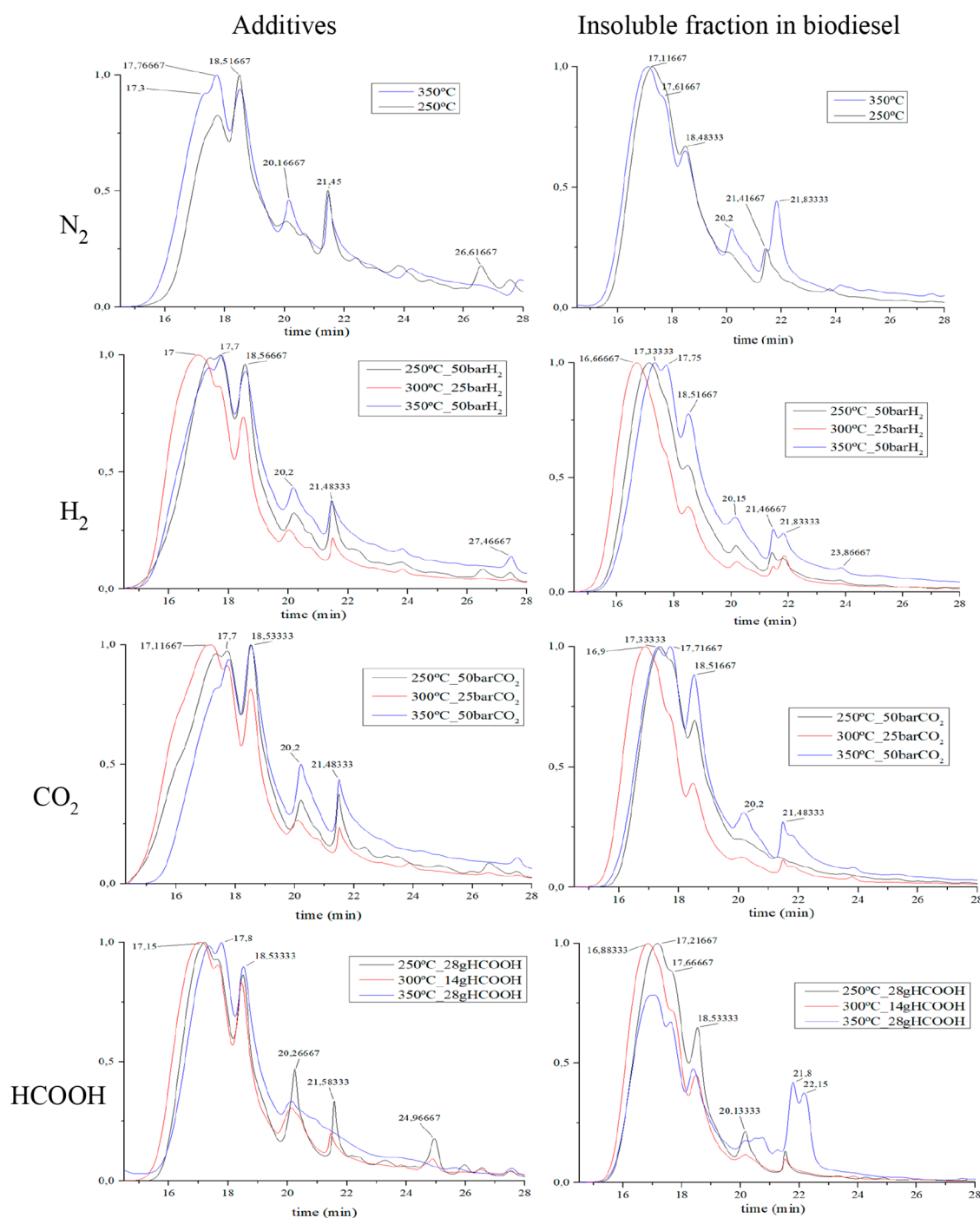


Figure 10. Molecular weight distribution (GPC plots) of the additives and their insoluble fractions in biodiesel.

7.6 at 250, 300, and 350 °C, respectively, which correlate with the decomposition extent of HCOOH.

It should be stressed that the GC–FID–MS analysis allowed for identifying and quantifying around 47% of the organic mass of the additive produced in the case of the inert atmosphere at 250 °C, a value that dropped to only 5% at 350 °C. The identified and quantified additive fraction obtained in the H₂ experiments dropped from 20% at 250 °C to 10% at higher temperatures and did not exceed 10% in the remaining cases. The identified fraction of additives constituted phenolic compounds (Table 5) and non-phenolic compounds, such as hexadecanoic acid methyl ester, acetic acid, and cyclopentenone derivatives.

The most important part of the GC–FID unquantified components could be related to undetectable phenolic dimers, trimers, and oligomers with a mass-to-charge index (m/z) higher than 500, also including repolymerized fractions of lignin with a very high molecular weight. For further characterization, the molecular weight distribution of the additives was analyzed (section 3.5.3).

3.5.2. FTIR Analysis of the Additives. FTIR spectra of the produced additives and that of the original raw material are represented in Figure 9. In general, the spectra show some significant differences in the function of the reaction medium and the lignin processing temperature. The peak intensity corresponding to the hydroxyl group (at wavenumbers in the

Table 6. Molecular Weight (M_n , M_w , and M_w/M_n) of the Whole Additives and Their Insoluble Fractions in Biodiesel

	T ($^{\circ}\text{C}$)	initial gas pressure (bar)/HCOOH weight (g)	whole additives			insoluble fraction of the additives in biodiesel		
			M_n (Da)	M_w (Da)	M_w/M_n	M_n (Da)	M_w (Da)	M_w/M_n
inert atmosphere experiments	250	0	6700	13000	1.9	10600	16800	1.6
	350	0	8200	15900	2.0	10700	18600	1.8
H_2 experiments	250	50	10000	18900	1.9	11800	18500	1.6
	350	50	9200	18400	2.0	9200	15900	1.7
	300	25	13200	22000	1.7	15600	23600	1.5
CO_2 experiments	250	50	12600	24700	2.0	9800	14600	1.5
	350	50	8100	16300	2.0	9300	15400	1.6
	300	25	15200	27300	1.8	14200	20700	1.4
HCOOH experiments	250	28	10000	16400	1.6	12600	17800	1.4
	350	28	9300	15100	1.6	10800	18700	1.7
	300	14	12000	19600	1.6	14600	20600	1.4

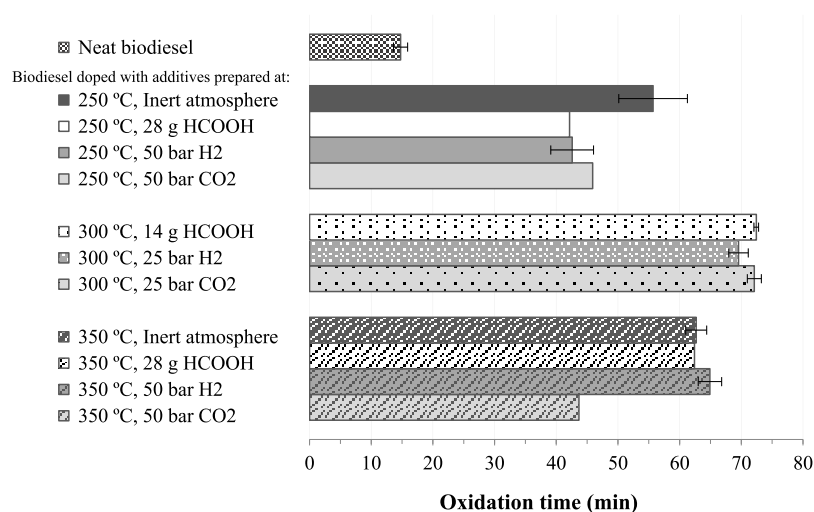


Figure 11. Oxidation stability times of neat and doped biodiesels.

range of $3600\text{--}3100\text{ cm}^{-1}$) was not strongly affected by the medium and/or the temperature but was more pronounced in the case of CO_2 and HCOOH medium. Peaks corresponding to alkyl groups (wavenumber between 3000 and 2900 cm^{-1}) almost completely disappeared in the additives obtained at $350\text{ }^{\circ}\text{C}$, regardless of the reaction medium. No peaks were detected throughout the interval of $3600\text{--}2900\text{ cm}^{-1}$ in the spectra of the original raw material. On the other hand, the two clear peaks observed in the original raw material at wavenumbers in the range of $1700\text{--}400\text{ cm}^{-1}$ have undergone several changes compared to the spectra of the additives obtained at $250\text{ }^{\circ}\text{C}$. Some of these peaks were reduced or disappeared, while others appeared when increasing the depolymerization temperature up to $300\text{ }^{\circ}\text{C}$, thus indicating the ASL_f depolymerization by cleavage of many functional groups and restructuration into other bonds. At $350\text{ }^{\circ}\text{C}$, the spectra of all of the additives became similar to char and activated carbon plots, with fewer peaks representing functional groups, which could indicate the condensation of phenolic compounds forming a residual or repolymerized lignin at this severe treatment temperature. It is noteworthy that, in the additives produced at 250 and $300\text{ }^{\circ}\text{C}$ (regardless of the reaction medium), an important peak appeared at wavenumbers of around $1300\text{--}1150\text{ cm}^{-1}$, with a significant shoulder at 1250 cm^{-1} . The peaks at these wavenumbers are usually attributed to aromatic links and tertiary/secondary alcohols, which could be explained by the

presence of catechol, alkyl catechol, syringol, guaiacol, and hydroquinone in the additives prepared at $300\text{ }^{\circ}\text{C}$ (Table 5). The intensity of the peak observed in the spectra of ASL_f at a wavenumber of around 1400 cm^{-1} (corresponding to O-CH_3 links) started to decrease in the additives prepared at $250\text{ }^{\circ}\text{C}$ in the presence of H_2 and CO_2 and almost completely disappeared at $300\text{ }^{\circ}\text{C}$. According to Li et al.,⁴⁹ the $\beta\text{-O-4}$ linkages are the first to be cleaved during the hydrothermal treatment. This peak was observed to reappear again in the additives produced at $350\text{ }^{\circ}\text{C}$ under a CO_2 medium and inert atmosphere, which might be due to repolymerization reactions involving linkages between phenolic rings, similar to those present in the original feedstock. No peaks were detected at this wavenumber (1400 cm^{-1}) in the additives produced at the highest temperature in the presence of HCOOH and H_2 , which seems to indicate that these H-donating reaction medium led to other types of products and could also be more efficient in preventing repolymerization reactions to avoid the formation of residual lignin. As commented, this effect on the insoluble solid yield was hindered because of experimental measurement uncertainty.

3.5.3. Molecular Weight Distribution of the Additives. The GPC chromatograms of both the entire additives and the insoluble fractions in biodiesel are reported in Figure 10. Table 6 summarizes final results, such as the number-average molecular weight (M_n), weight-average molecular weight

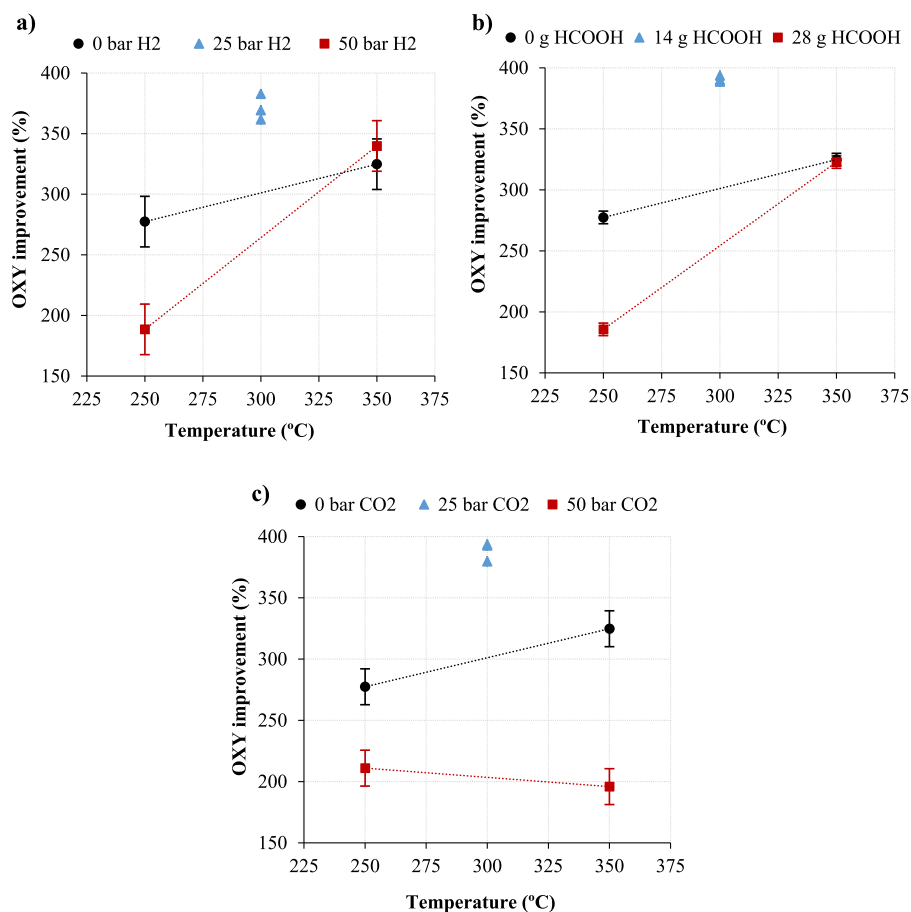


Figure 12. Effect of the temperature and reagent amount used in the depolymerization experiments on the improvement of biodiesel oxidation stability: (a) H₂ experiments, (b) HCOOH experiments, and (c) CO₂ experiments.

(M_w), and polydispersity (M_w/M_n) of the analyzed samples. As shown in Figure 10, up to four different peaks (or shoulders) were observed for the additives. The peaks that eluted at lower retention times could be related to a part of unconverted lignin, higher molecular weight fragments of lignin, and repolymerized lignin, while the peaks observed at a higher retention time (from 21 min) are associated with a lower molecular weight (<1400 Da), thus meaning that the depolymerization reaction had occurred to a greater or lesser extent.²⁹ Noteworthy is the significant increase in peaks at a retention time of around 17 min in the additives produced at 300 °C, regardless of the reaction atmosphere, which indicates a higher molecular weight compared to those obtained at 250 and 350 °C. This tendency was also observed in the non-soluble additive fraction (probably because of repolymerization reactions). The comparison of the GPC plots of the entire additives and their respective insoluble fractions in biodiesel highlights a noticeable decrease in the intensities of the peaks at retention times of 18.5, 20.2, and 21.48. This reduction is related to the fraction of the additive that was mainly dissolved in biodiesel. These soluble compounds include molecules with a molecular size of <1400 Da and a heavier fraction with a molecular weight of around 7000 Da (more noticeable in the additives obtained at 300 °C under all reaction medium).

Concerning the global data of M_n and M_w , higher values were obtained for either the entire additive or the fraction insoluble in biodiesel depending upon the depolymerization operating conditions. The better solubility of the additives has

been correlated with a higher molecular weight of the insoluble fractions compared to the entire additive, thus pointing to a prevalence of the smaller molecules in the fraction of the additive soluble in biodiesel. Moreover, it should be noted that the incorporation of H₂, CO₂, or HCOOH to the reaction medium had a noticeable effect on increasing the molecular weight of the additives, especially at 350 °C.

3.6. Oxidation Stability of Biodiesel. Figure 11 shows a visual comparison of all of the results of biodiesel oxidation stability time (PetroOXY tests). The average oxidation stability time (OXY) of neat biodiesel was 14.8 ± 1.1 min. As a general result, doping biodiesel with ASL lignin-based additives has been demonstrated to achieve an excellent improvement of the OXY time. More specifically, increasing the depolymerization temperature from 250 to 300 °C resulted in a significant increase in the OXY time, while only slight differences were observed as a result of the reaction medium for ASL_f depolymerization at this temperature. However, the results obtained at 250 and 350 °C were more affected by the reaction medium. To examine the impact of the factors on this response, the ANOVA statistical analysis was performed on the improvement rate of the OXY time (eq 5).

$$\text{OXY improvement (\%)} = \frac{\text{OXY doped biodiesel} - \text{OXY neat biodiesel}}{\text{OXY neat biodiesel}} \times 100 \quad (5)$$

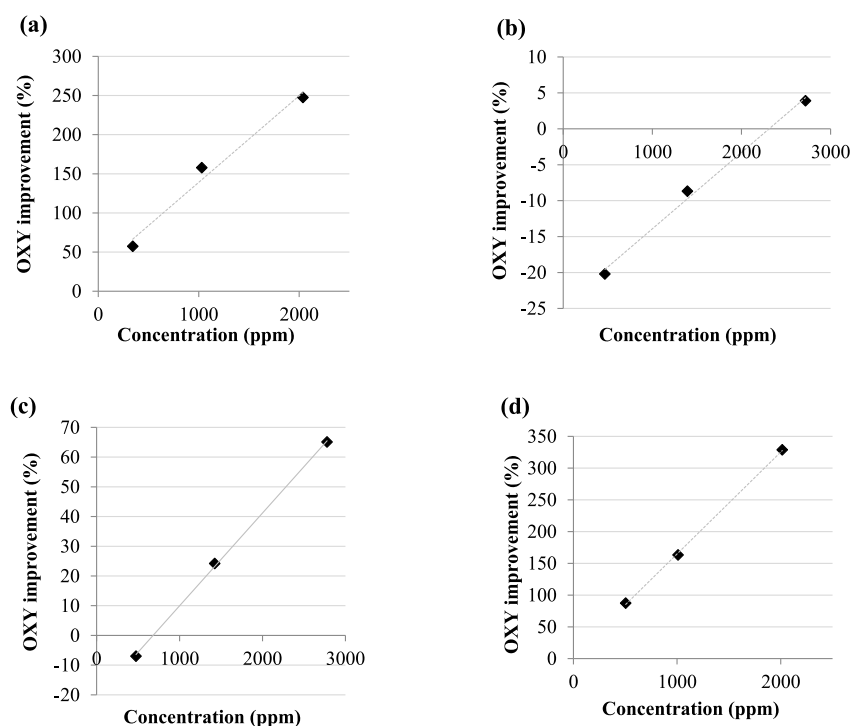


Figure 13. Improvement of biodiesel oxidation stability as a function of the concentrations of (a) catechol, (b) guaiacol, (c) syringol, and (d) BKF dimer.

The results from ANOVA (Figure 12) indicate that both the temperature and the reaction medium and the interaction between them were significant terms in all cases. The increase in the reaction temperature from 250 to 350 °C had a positive impact on the biodiesel oxidation stability achieved with the additives obtained under an inert atmosphere or H₂ and HCOOH medium but not in the case of the CO₂ medium (similar results for both temperatures). However, experimental data did not fit a linear model, but a strong curvature was detected at 300 °C, regardless of the nature of the reagent incorporated (quadratic effect of the temperature). On the other hand, introducing H₂ or HCOOH in the process was not an advantage for this studied variable. No substantial differences were found at the highest temperatures (300–350 °C), obtaining similar oxidation stability values in the three cases (with or without adding H₂ or HCOOH). However, at a temperature of 250 °C, a negative effect of the presence of H₂ (50 bar) or HCOOH (28 g) was even observed when comparing to the result obtained in the inert atmosphere. These results seem to be connected with the observed decrease in the additive solubility in biodiesel, which dropped from a real soluble dosage of 0.74 wt % for the additive produced under an inert atmosphere to 0.4 and 0.61 wt % for the additives produced under H₂ and HCOOH medium, respectively. On the other hand, adding 50 bar of CO₂ to the reaction medium led to additives that achieved lower OXY improvements than those obtained in the N₂ inert atmosphere. Concretely, the improvement of oxidation stability decreased dramatically from 334% (with the additive obtained in a N₂ atmosphere at 350 °C) to 196% (with the additive produced at 350 °C and 50 bar of CO₂), while in H₂ and HCOOH medium, such variation was not observed (OXY improvement of 340 and 323%, respectively). Therefore, the most favorable operating conditions from the point of view of maximizing the improvement of biodiesel oxidation stability

were those corresponding to the central points of the experimental design: 391% (300 °C and 28 g of HCOOH), 389% (300 °C and 25 bar of CO₂), and 371% (300 °C and 25 bar of H₂).

The composition of the additives analyzed by GC–FID–MS (Table 5) can partially help to explain the trends observed in the antioxidant potential of the additives. For instance, the highest concentration of catechol was obtained at a treatment temperature of 300 °C, regardless of the reaction medium. This finding could also be related to obtaining the maximum improvement rate of the oxidation stability with the additives produced at 300 °C. Catechol has been reported to show a high antioxidant potential, even at lower dosages,^{35,51} much higher than other phenolic monomers derived from lignin, such as guaiacol or alkylated guaiacols, that not only do not have an antioxidant effect but, instead, have a pro-oxidant effect.³⁵ That means that the presence of guaiacols could play a role in the dilution of the antioxidant activity of other active components present in the additives, such as catechol.

Additionally, Larson et al. reported that not only monomers but also dimers and oligomers obtained from lignin fractionation have a great antioxidant activity,³⁵ even though they were hard to determine, which is the nature of these components by GC–MS analysis. Hence, the antioxidant capacity of the additives produced in this study could be affected too by the presence of dimers and oligomers undetected by GC–MS, especially because the results of the GPC tests showed that the *M_w* of the additives produced were in the order of 15 000 Da and the size of the fraction soluble in biodiesel was mainly lower than 7000 Da. Dimer potential candidates in ASL_f depolymerization could be based on monomers of catechol or guaiacol, such as α,ω -dicatechols or diguaiacols, and both proved to have an important antioxidant activity.³⁵

With the aim to study the individual effect of some phenolic compounds in the oxidation stability of biodiesel, biodiesel was blended with catechol, syringol, guaiacol, and a dimer commercially named as the BKF antioxidant [2,2'-methylenebis(4-methyl-6-*tert*-butylphenol, whose structure is shown in Figure S4 of the Supporting Information] at different concentrations, and OXY tests were conducted according to the same methodology used before. Figure 13 shows the biodiesel OXY improvement as a function of the phenolic compound concentration. As shown, both catechol and the BKF antioxidant positively and linearly affect the oxidation stability, even at a low concentration. In contrast, the inverse trend was shown in the case of guaiacol, negatively affecting the oxidation, which confirms the pro-oxidant effect of this component. Similar to guaiacol, syringol negatively affects the oxidation stability of biodiesel at a low concentration but slightly improves it at higher dosages. These results correlate with the finding that the additives with a higher catechol content and lower guaiacol/guaiacol derivate content led to the most remarkable OXY improvements.

CONCLUSION

Depolymerization of lignin extracted from argan shells to produce added-value chemicals, specifically antioxidant additives, has been studied. Lignin from argan shells was processed in hydrothermal conditions under N₂, H₂, CO₂, or HCOOH as the reaction medium at temperatures ranging from 250 to 350 °C. For the purpose of producing antioxidant additives for biofuels, such as biodiesel, the depolymerization temperature was a critical factor in both the production and antioxidant potential and solubility of the additives. In general, a significant increase in the biodiesel oxidation stability time was obtained at a small dosage of additive (<1 wt %). Under the best operating conditions (300 °C), the process yielded 15–20% of additive and the improvement of the oxidation stability of biodiesel doped with these additives was close to 400%, regardless of the reaction medium. The presence of catechol and catechol derivatives in the additives obtained at 300 °C could be partially responsible for these good results of oxidation stability. This experimental study has shown the technical feasibility to produce efficient antioxidant additives from an underused waste, such as argan shell. However, more effort is required to develop a simpler process that could be economically feasible at a larger scale in the context of a biorefinery process focused on argan uses.

ASSOCIATED CONTENT

Supporting Information

The Supporting Information is available free of charge at <https://pubs.acs.org/doi/10.1021/acs.energyfuels.1c01705>.

Operating and method parameters used in the GC–FID–MS analysis of the produced additives (Table S1), maximal pressures reached during the depolymerization experiments in a Parr reactor at different operational conditions (Table S2), elemental analysis of the insoluble and soluble solids (Table S3), distribution of C, H, and N in soluble and insoluble solids (Table S4), pH values of the reaction mixture before and after each experiment (Table S5), GPC standards and calibration curve (Figure S1), residual gas pressure in the reactor (measured at 20 °C) (Figure S2), joint yield of soluble and insoluble solids from depolymerization experiments

(Figure S3), and structure of the BKF antioxidant (Figure S4) (PDF)

AUTHOR INFORMATION

Corresponding Author

Jesús Arauzo – Thermochemical Processes Group, Aragón Institute of Engineering Research (I3A), University of Zaragoza, 50018 Zaragoza, Spain; orcid.org/0000-0002-5959-3168; Email: jarauzo@unizar.es

Authors

Zainab Afailal – Thermochemical Processes Group, Aragón Institute of Engineering Research (I3A), University of Zaragoza, 50018 Zaragoza, Spain

Noemí Gil-Lalaguna – Thermochemical Processes Group, Aragón Institute of Engineering Research (I3A), University of Zaragoza, 50018 Zaragoza, Spain; orcid.org/0000-0002-8704-9274

María Teresa Torrijos – Thermochemical Processes Group, Aragón Institute of Engineering Research (I3A), University of Zaragoza, 50018 Zaragoza, Spain

Alberto Gonzalo – Thermochemical Processes Group, Aragón Institute of Engineering Research (I3A), University of Zaragoza, 50018 Zaragoza, Spain

José Luis Sánchez – Thermochemical Processes Group, Aragón Institute of Engineering Research (I3A), University of Zaragoza, 50018 Zaragoza, Spain; orcid.org/0000-0002-9705-2207

Complete contact information is available at: <https://pubs.acs.org/10.1021/acs.energyfuels.1c01705>

Author Contributions

Zainab Afailal, investigation and writing the original draft and editing; Noemí Gil-Lalaguna, methodology and writing reviewing and editing; María Teresa Torrijos, investigation; Alberto Gonzalo, technical support and writing reviewing and editing; Jesús Arauzo, supervision; and José Luis Sánchez, scientific work and writing reviewing and editing.

Notes

The authors declare no competing financial interest.

ACKNOWLEDGMENTS

The authors express their gratitude to the Aragón government (Research Group T22_20R), co-funded by FEDER 2014–2020 “Construyendo Europa desde Aragón”, and MINECO (Project ENE2017-85040-R: Renewable Additives for Biofuels) for providing the frame support of this work.

REFERENCES

- (1) Effendi, A.; Gerhauser, H.; Bridgwater, A. V. Production of renewable phenolic resins by thermochemical conversion of biomass: A review. *Renewable Sustainable Energy Rev.* **2008**, *12* (8), 2092–2116.
- (2) Pandey, M. P.; Kim, C. S. Lignin Depolymerization and Conversion: A Review of Thermochemical Methods. *Chem. Eng. Technol.* **2011**, *34* (1), 29–41.
- (3) Amen-Chen, C.; Pakdel, H.; Roy, C. Production of monomeric phenols by thermochemical conversion of biomass: A review. *Bioresour. Technol.* **2001**, *79* (3), 277–299.
- (4) Gillet, S.; Aguedo, M.; Petitjean, L.; Morais, A. R. C.; da Costa Lopes, A. M.; Łukasik, R. M.; Anastas, P. T. Lignin transformations for high value applications: Towards targeted modifications using green chemistry. *Green Chem.* **2017**, *19* (18), 4200–4233.

- (5) Lavoie, J.-M.; Ghislain, T.; Bahl, E.; Arauzo, J.; Gonzalo, A.; Gil-Lalaguna, N.; Sánchez, J. L. Renewable antioxidant additive for biodiesel obtained from black liquor. *Fuel* **2019**, *254*, 115689.
- (6) Tolbert, A.; Akinosho, H.; Khunsupat, R.; Naskar, A. K.; Ragauskas, A. J. Characterization and analysis of the molecular weight of lignin for biorefining studies. *Biofuels, Bioprod. Biorefin.* **2014**, *8* (6), 836–856.
- (7) Huang, S.; Mahmood, N.; Tymchyshyn, M.; Yuan, Z.; Xu, C. Reductive de-polymerization of kraft lignin for chemicals and fuels using formic acid as an in-situ hydrogen source. *Bioresour. Technol.* **2014**, *171*, 95–102.
- (8) da Costa Sousa, L.; Jin, M.; Chundawat, S. P. S.; Bokade, V.; Tang, X.; Azarpira, A.; Lu, F.; Avci, U.; Humpala, J.; Uppugundla, N.; Gunawan, C.; Pattathil, S.; Cheh, A. M.; Kothari, N.; Kumar, R.; Ralph, J.; Hahn, M. G.; Wyman, C. E.; Singh, S.; Simmons, B. A.; Dale, B. E.; Balan, V. Next-generation ammonia pretreatment enhances cellulosic biofuel production. *Energy Environ. Sci.* **2016**, *9* (4), 1215–1223.
- (9) Morais, A. R. C.; Pinto, J. V.; Nunes, D.; Roseiro, L. B.; Oliveira, M. C.; Fortunato, E.; Bogel-Lukasik, R. Imidazole: Prospect Solvent for Lignocellulosic Biomass Fractionation and Delignification. *ACS Sustainable Chem. Eng.* **2016**, *4* (3), 1643–1652.
- (10) Gonzalo, A.; Bimbela, F.; Sánchez, J. L.; Labidi, J.; Marín, F.; Arauzo, J. Evaluation of different agricultural residues as raw materials for pulp and paper production using a semichemical process. *J. Cleaner Prod.* **2017**, *156*, 184–193.
- (11) Marín, F.; Sánchez, J. L.; Arauzo, J.; Fuertes, R.; Gonzalo, A. Semichemical pulping of *Miscanthus giganteus*. *Bioresour. Technol.* **2009**, *100* (17), 3933–3940.
- (12) Ragauskas, A. J.; Beckham, G. T.; Bidy, M. J.; Chandra, R.; Chen, F.; Davis, M. F.; Davison, B. H.; Dixon, R. A.; Gilna, P.; Keller, M.; Langan, P.; Naskar, A. K.; Saddler, J. N.; Tschaplinski, T. J.; Tuskan, G. A.; Wyman, C. E. Lignin Valorization: Improving Lignin Processing in the Biorefinery. *Science* **2014**, *344* (6185), 1246843.
- (13) Beauchet, R.; Monteil-Rivera, F.; Lavoie, J. M. Conversion of lignin to aromatic-based chemicals (L-chems) and biofuels (L-fuels). *Bioresour. Technol.* **2012**, *121*, 328–334.
- (14) Kang, S.; Li, X.; Fan, J.; Chang, J. Hydrothermal conversion of lignin: A review. *Renewable Sustainable Energy Rev.* **2013**, *27*, 546–558.
- (15) Cao, L.; Yu, I. K. M.; Liu, Y.; Ruan, X.; Tsang, D. C. W.; Hunt, A. J.; Ok, Y. S.; Song, H.; Zhang, S. Lignin valorization for the production of renewable chemicals: State-of-the-art review and future prospects. *Bioresour. Technol.* **2018**, *269*, 465–475.
- (16) Garrote, G.; Domínguez, H.; Parajó, J. C. Hydrothermal processing of lignocellulosic materials. *Holz als Roh- und Werkstoff.* **1999**, *57* (3), 191–202.
- (17) Akhtar, J.; Amin, N. A. S. A review on process conditions for optimum bio-oil yield in hydrothermal liquefaction of biomass. *Renewable Sustainable Energy Rev.* **2011**, *15* (3), 1615–1624.
- (18) Gosselink, R. J. A.; Teunissen, W.; van Dam, J. E. G.; de Jong, E.; Gellerstedt, G.; Scott, E. L.; Sanders, J. P. M. Lignin depolymerisation in supercritical carbon dioxide/acetone/water fluid for the production of aromatic chemicals. *Bioresour. Technol.* **2012**, *106*, 173–177.
- (19) Otromke, M.; White, R. J.; Sauer, J. Hydrothermal base catalyzed depolymerization and conversion of technical lignin—An introductory review. *Carbon Resources Conversion.* **2019**, *2* (1), 59–71.
- (20) He, W.; Li, G.; Kong, L.; Wang, H.; Huang, J.; Xu, J. Application of hydrothermal reaction in resource recovery of organic wastes. *Resour., Conserv. Recycl.* **2008**, *52* (5), 691–699.
- (21) Chandrasekaran, S. R.; Murali, D.; Marley, K. A.; Larson, R. A.; Doll, K. M.; Moser, B. R.; Scott, J.; Sharma, B. K. Antioxidants from Slow Pyrolysis Bio-Oil of Birch Wood: Application for Biodiesel and Biobased Lubricants. *ACS Sustainable Chem. Eng.* **2016**, *4* (3), 1414–1421.
- (22) Davoudzadeh, F.; Smith, B.; Avni, E.; Coughlin, R. W. Depolymerization of lignin at low pressure using lewis acid catalysts and under high pressure using H₂ donor solvents. *Holzforschung* **1985**, *39* (3), 159–166.
- (23) Kleinert, M.; Gasson, J. R.; Barth, T. Optimizing solvolysis conditions for integrated depolymerisation and hydrodeoxygenation of lignin to produce liquid biofuel. *J. Anal. Appl. Pyrolysis* **2009**, *85* (1), 108–117.
- (24) Kim, K. H.; Brown, R. C.; Kieffer, M.; Bai, X. Hydrogen-Donor-Assisted Solvent Liquefaction of Lignin to Short-Chain Alkylphenols Using a Micro Reactor/Gas Chromatography System. *Energy Fuels* **2014**, *28* (10), 6429–6437.
- (25) Scanlon, J. T.; Willis, D. E. Calculation of Flame Ionization Detector Relative Response Factors Using the Effective Carbon Number Concept. *J. Chromatogr. Sci.* **1985**, *23* (8), 333–340.
- (26) Mahmood, N.; Yuan, Z.; Schmidt, J.; Xu, C. Production of polyols via direct hydrolysis of kraft lignin: Effect of process parameters. *Bioresour. Technol.* **2013**, *139*, 13–20.
- (27) Toledano, A.; Serrano, L.; Labidi, J. Improving base catalyzed lignin depolymerization by avoiding lignin repolymerization. *Fuel* **2014**, *116*, 617–624.
- (28) Erdocia, X.; Prado, R.; Corcuera, M. Á.; Labidi, J. Base catalyzed depolymerization of lignin: Influence of organosolv lignin nature. *Biomass Bioenergy* **2014**, *66*, 379–386.
- (29) Toledano, A.; Serrano, L.; Labidi, J. Organosolv lignin depolymerization with different base catalysts. *J. Chem. Technol. Biotechnol.* **2012**, *87* (11), 1593–1599.
- (30) Zabaleta, A. T. Lignin extraction, purification and depolymerization study. Ph.D. Thesis, Departamento de Ingeniería Química y del Medio Ambiente, Universidad del País Vasco, San Sebastián, Spain, 2012.
- (31) Kähkönen, M. P.; Hopia, A. I.; Vuorela, H. J.; Rauha, J.-P.; Pihlaja, K.; Kujala, T. S.; Heinonen, M. Antioxidant Activity of Plant Extracts Containing Phenolic Compounds. *J. Agric. Food Chem.* **1999**, *47* (10), 3954–3962.
- (32) Yaakob, Z.; Narayanan, B. N.; Padikkaparambil, S.; Unni, K. S.; Akbar, P. M. A review on the oxidation stability of biodiesel. *Renewable Sustainable Energy Rev.* **2014**, *35*, 136–153.
- (33) Tabatabaei, M.; Aghbashlo, M. The critical role of advanced sustainability assessment tools in enhancing the real-world application of biofuels. *Acta Innovations* **2020**, *37*, 67–73.
- (34) Pullen, J.; Saeed, K. An overview of biodiesel oxidation stability. *Renewable Sustainable Energy Rev.* **2012**, *16* (8), 5924–5950.
- (35) Larson, R. A.; Sharma, B. K.; Marley, K. A.; Kunwar, B.; Murali, D.; Scott, J. Potential antioxidants for biodiesel from a softwood lignin pyrolyzate. *Ind. Crops Prod.* **2017**, *109*, 476–482.
- (36) Domingos, A. K.; Saad, E. B.; Vechiatto, W. W. D.; Wilhelm, H. M.; Ramos, L. P. The influence of BHA, BHT and TBHQ on the oxidation stability of soybean oil ethyl esters (biodiesel). *J. Braz. Chem. Soc.* **2007**, *18*, 416–423.
- (37) Focke, W. W.; van der Westhuizen, I.; Grobler, A. B. L.; Nshoane, K. T.; Reddy, J. K.; Luyt, A. S. The effect of synthetic antioxidants on the oxidative stability of biodiesel. *Fuel* **2012**, *94*, 227–233.
- (38) Gil-Lalaguna, N.; Bautista, A.; Gonzalo, A.; Sánchez, J. L.; Arauzo, J. Obtaining biodiesel antioxidant additives by hydrothermal treatment of lignocellulosic bio-oil. *Fuel Process. Technol.* **2017**, *166*, 1–7.
- (39) Palomo, J.; Moles, S.; Salafranca, J.; Gil-Lalaguna, N.; Gonzalo, A.; Sánchez, J. L. Production of antioxidants for biodiesel from straw black liquor depolymerization. *WIT Trans. Ecol. Environ.* **2019**, *237*, 97–108.
- (40) Botella, L.; Stankovikj, F.; Sánchez, J. L.; Gonzalo, A.; Arauzo, J.; García-Pérez, M. Bio-Oil Hydrotreatment for Enhancing Solubility in Biodiesel and the Oxidation Stability of Resulting Blends. *Front. Chem.* **2018**, *6*, 83–83.
- (41) García, M.; Botella, L.; Gil-Lalaguna, N.; Arauzo, J.; Gonzalo, A.; Sánchez, J. L. Antioxidants for biodiesel: Additives prepared from extracted fractions of bio-oil. *Fuel Process. Technol.* **2017**, *156*, 407–414.

(42) Manzanares, P. The role of biorefining research in the development of a modern bioeconomy. *Acta Innovations*. **2020**, *37*, 47–56.

(43) Kállai, M.; Balla, J. The effect of molecular structure upon the response of the flame ionization detector. *Chromatographia* **2002**, *56* (5), 357–360.

(44) Jorgensen, A. D.; Picel, K. C.; Stamoudis, V. C. Prediction of gas chromatography flame ionization detector response factors from molecular structures. *Anal. Chem.* **1990**, *62* (7), 683–689.

(45) Tedsree, K.; Li, T.; Jones, S.; Chan, C. W. A.; Yu, K. M. K.; Bagot, P. A. J.; Marquis, E. A.; Smith, G. D. W.; Tsang, S. C. E. Hydrogen production from formic acid decomposition at room temperature using a Ag-Pd core-shell nanocatalyst. *Nat. Nanotechnol.* **2011**, *6* (5), 302–307.

(46) Yuan, Z.; Cheng, S.; Leitch, M.; Xu, C. Hydrolytic degradation of alkaline lignin in hot-compressed water and ethanol. *Bioresour. Technol.* **2010**, *101* (23), 9308–9313.

(47) Long, J.; Xu, Y.; Wang, T.; Shu, R.; Zhang, Q.; Zhang, X.; Fu, J.; Ma, L. Hydrothermal Depolymerization of Lignin: Understanding the Structural Evolution. *BioResources* **2014**, *9* (4), 7162–7175.

(48) Miller, J.; Evans, L.; Mudd, J.; Brown, K. *Batch Microreactor Studies of Lignin Depolymerization by Bases. 2. Aqueous Solvents*; Sandia National Laboratories: Albuquerque, NM, 2002; Technical Report SAND2002-1318.

(49) Li, J.; Henriksson, G.; Gellerstedt, G. Lignin depolymerization/repolymerization and its critical role for delignification of aspen wood by steam explosion. *Bioresour. Technol.* **2007**, *98* (16), 3061–3068.

(50) Kleinert, M.; Barth, T. Phenols from lignin. *Chem. Eng. Technol.* **2008**, *31* (5), 736–745.

(51) Botella, L.; Bimbela, F.; Martín, L.; Arauzo, J.; Sánchez, J. L. Oxidation stability of biodiesel fuels and blends using the Rancimat and PetroOXY methods. Effect of 4-allyl-2,6-dimethoxyphenol and catechol as biodiesel additives on oxidation stability. *Front. Chem.* **2014**, *2*, 43.